Mathematical Biosciences and Engineering

https://www.aimspress.com/journal/mbe

MBE, 22(12): 3107–3129.
DOI: 10.3934/mbe.2025115
Received: 25 July 2025
Revised: 13 October 2025
Accepted: 16 October 2025
Published: 24 October 2025

Research article

Environmental variability and fish stock dynamics: a stochastic model of Mahi Mahi abundance

Erika Johanna Martínez-Salinas[1], Andrés Ríos-Gutiérrez[1,2], Viswanathan Arunachalam[1,*] and John Josephraj Selvaraj[3]

[1] Department of Statistics, Universidad Nacional de Colombia, Sede Bogotá, Colombia
[2] School of Mathematics, Universidad Industrial de Santander, Bucaramanga, Colombia
[3] Faculty of Engineering and Administration, Universidad Nacional de Colombia, Sede Palmira, Colombia

* **Correspondence:** Email: varunachalam@unal.edu.co.

Abstract: Climatic factors exert a substantial influence on both biotic and abiotic components of marine ecosystems, significantly affecting the abundance and spatial distribution of fish species. In this study, we introduced a stochastic modeling framework, grounded in stochastic differential equations (SDEs), to analyze the temporal dynamics of sea surface temperature and its relationship with the abundance of Mahi Mahi (*Coryphaena hippurus*) in a region of the Colombian Pacific coast. Model parameters such as sea surface temperature, fish stock, and catch per unit effort for the period 2000 to 2012 were estimated using the maximum likelihood method, implemented via the Euler–Maruyama numerical scheme. The model's performance was assessed using empirical data through numerical simulation, cross-validation, and sensitivity analysis, demonstrating its applicability and robustness in capturing key ecological dynamics.

Keywords: stochastic differential equations; Ornstein-Uhlenbeck process; catch per unit of effort; maximum likelihood estimation; Euler-Maruyama method

1. Introduction

Fishing along the Colombian Pacific coast requires a variety of methods and gear, and is a primary source of livelihood for many coastal communities [1]. According to the 2007 report by the Intergovernmental Panel on Climate Change (IPCC), small-scale fisheries are among the sectors most vulnerable to the impacts of climate change [2]. Given their strategic and socioeconomic importance, ensuring the sustainability of these fisheries under increasing climate variability is of critical urgency. Countries such as Colombia, Ecuador, Bolivia, and Panama are particularly at risk due to rising sea

surface temperatures (SST), which threaten marine biodiversity and the availability of fishery resources.

Rising SST alters the physicochemical properties of marine ecosystems, thereby affecting the abundance, distribution, and harvest potential of fish species. Marine population dynamics are inherently stochastic, as evidenced by biological, ecological, and economic research. Markov chains have been employed to model fish population dynamics and to better understand system behavior under uncertainty [3]. In parallel, stochastic economic growth models, such as those developed by Merton [4] and Pindyck [5], have incorporated random processes to describe labor dynamics and natural resource use [6].

Climate change fundamentally shifts environmental baselines, significantly altering the spatial and temporal distribution of marine species. Analyzing recent temperature trends and their effects on species dynamics is therefore essential. For example, the researchers in [7] examined the combined effects of climate variability, fishing pressure, and endogenous biological processes on anchovy and sardine populations off the Chilean coast. Their results highlight SST as a primary driver of sardine biomass, especially after 2006, underscoring the importance of incorporating climate variability into fisheries management strategies.

A number of models have been proposed to characterize temperature fluctuations. Barboza et al. [8] used Bayesian methods to reconstruct anomalies in land and sea temperatures. Dornier and Queruel [9] employed regression models with seasonal adjustments and sinusoidal trends to account for global warming effects. Brody et al. [10] modeled temperature dynamics using fractional Brownian motion, where the Hurst parameter $H \in (0, 1)$ captures the system's tendency to revert toward seasonal norms. In a different context, [11] modeled daily temperature in Balaka, Africa, using the Ornstein-Uhlenbeck process. Additionally, [10] explored skewed, heavy-tailed inverse-normal distributions to model temperature variability. These diverse modeling strategies reflect the complexity of temperature dynamics and their ecological implications.

Global climate projections indicate declines in species richness and abundance, alongside changes in key oceanographic variables, with direct consequences for global fisheries [12]. In Colombia, despite the country's rich fishery resources, the relationship between climate factors and fishery composition in the Pacific region remains understudied. Regulatory oversight has been inconsistent, in part due to the absence of a permanent fisheries authority, which has changed institutional homes multiple times since the 1990s [13]. Consequently, national fisheries data are fragmented. Nevertheless, historical catch records from 1950 to 2010 have been reconstructed using data from the Food and Agriculture Organization (FAO) [14, 15]. Although few researchers have assessed the impacts of climate change on Colombian fisheries [16], such research is critical for informing policy and safeguarding the livelihoods of coastal communities. The production of rigorous scientific evidence is essential for effective decision-making and the sustainable governance of marine resources.

In this study, we examined the impact of sea surface temperature variability on Mahi Mahi (*Coryphaena hippurus*) catch in the Colombian Pacific region. A stochastic modeling approach is proposed to capture the dynamic interactions among fish catch, stock abundance, and SST. The temperature component is modeled using an Ornstein-Uhlenbeck process, as formulated by [11], to reflect its mean-reverting stochastic behavior. Model parameters are estimated using the maximum likelihood method, and numerical integration is performed using the Euler-Maruyama scheme.

The remainder of this article is structured as follows: in Section 2, we introduce the conceptual framework and present the stochastic model incorporating random perturbations. In Section 3, we outline the parameter estimation methodology, followed by simulation results, forecasting, cross-validation, confidence interval construction, and sensitivity analysis. Finally, In Section 4, we summarize the key findings and offer directions for future research.

2. Stochastic model

In this section, we present a stochastic modeling framework designed to examine sea surface temperature (SST) variability and its influence on fishing dynamics, with particular emphasis on Mahi Mahi (*C. hippurus*) in the Colombian Pacific. The fishery data utilized for model development and validation were provided by the Hydrobiological Resources Research Group at the Universidad Nacional de Colombia, Sede Palmira, and by Sepúlveda Rodgers & Cía. Ltda. These data are not publicly available. The environmental dataset employed in this study is formatted in NetCDF, a widely adopted standard for representing multidimensional scientific variables, such as SST and salinity, where each dimension defines the structural organization of the data.

Mahi Mahi is of high commercial value for b artisanal and industrial fisheries in the region. It is typically harvested using surface longlines and handlines, while industrial pelagic fleets also employ surface gillnets during night operations [17]. According to the Autoridad Nacional de Acuicultura y Pesca (AUNAP), total landings along the Colombian Pacific coast amounted to 50 tonnes in 2013. This species forms large schools and inhabits both coastal and offshore waters, reaching depths of up to 85 meters. Due to its biological traits and market demand, Mahi Mahi has substantial exploitation potential. In 2014, the Colombian Ministry of Agriculture established a national quota of 2000 tonnes.

The model integrates oceanographic data, specifically sea surface temperature (SST), obtained from satellite-based passive sensors. These satellites provide global SST estimates, where each image pixel represents a spatially localized temperature value. Remote sensing data are fundamental for environmental monitoring and risk assessment. In addition to SST, the dataset includes fish catch records representing the number of individuals captured within the study area. The temporal resolution is daily and monthly, based on remote sensing sources. The dataset spans January 1979 to December 2012. Geospatial coordinates (latitude and longitude) define the spatial extent of the study region, as illustrated in Figure 1.

Researchers such as [18] and [19] have examined the effects of persistent temperature changes on marine ecosystems. In particular, the researchers in [17] report that fish catch is often correlated with temperature variability, depending on species-specific distributions. Motivated by these findings, we propose a model to characterize the behavior of SST and evaluate its implications for fisheries management.

We begin by analyzing the SST time series, in which each monthly observation comprises three representative statistical measures, maximum, minimum, and mean SST, calculated from all pixels within the study area for each satellite image. Figure 2 presents the mean SST time series derived from satellite observations spanning 1979–2012. The series exhibits pronounced variability and a consistent tendency to revert toward a long-term equilibrium, suggesting the presence of mean-reverting stochastic dynamics in sea surface temperature variability.

To assess the distributional properties of the SST data, we apply the Anderson-Darling test [20].

The null hypothesis H_0 assumes that the data follow a normal distribution. The test yields a statistic of $A = 1.1076$ with a p-value of 0.92166, indicating that H_0 cannot be rejected at the 5% significance level. We therefore conclude that the SST data are consistent with a normal distribution.

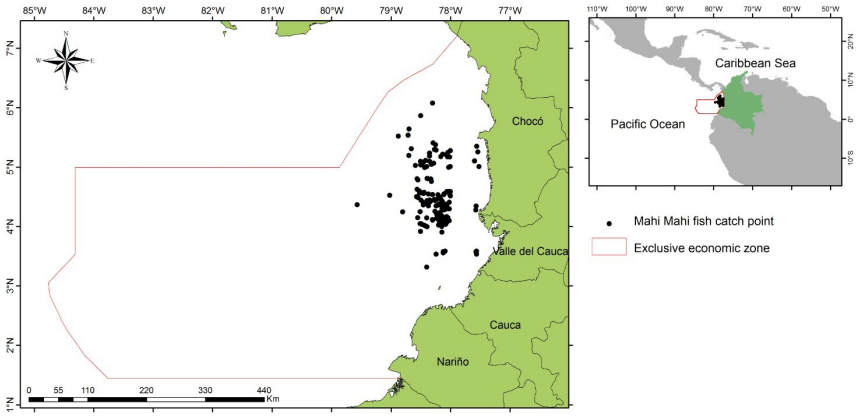

Figure 1. Geographic area of data collection for Mahi Mahi.

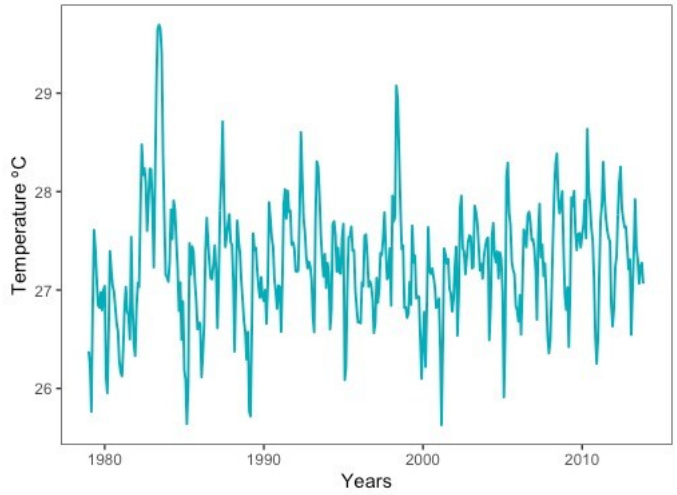

Figure 2. Observed mean sea surface temperature values (°C) in the study area.

Following the methodologies of [21], we model SST as an Ornstein-Uhlenbeck process with a time-dependent mean reversion level, denoted by θ_t. The process is defined to satisfy the expectation condition:

$$E[T_t] = \theta_t. \tag{2.1}$$

To ensure this condition holds, the OU process is specified as:

$$dT_t = \left[a(\theta_t - T_t) + \frac{d\theta_t}{dt}\right]dt + \sigma_t dB_t, \tag{2.2}$$

where $\{B_t\}_{t\geq 0}$ is a standard Brownian motion defined on a filtered probability space $(\Omega, \Im, P)$ with

filtration $\{\Im_t\}_{t\geq 0}$. The model parameters are: a: The speed of mean reversion, θ_t: The time-varying long-term mean, σ_t: The temperature volatility, and $\frac{d\theta_t}{dt}$.

To understand fish population dynamics, we first consider the deterministic logistic growth model proposed by Verhulst:

$$\frac{dX_t}{dt} = X_t r\left(1 - \frac{X_t}{k}\right), \tag{2.3}$$

where X_t denotes the fish population at time t, r is the intrinsic growth rate, and k is the environmental carrying capacity. Catch volume alone does not fully represent fish population dynamics, as it is influenced by multiple factors, including biomass availability, fishing effort, gear selectivity, and environmental variability [22]. When harvesting is incorporated, the catch at time t is defined as:

$$H_t = \beta X_t Y_t, \tag{2.4}$$

where X_t is the stock size, Y_t is the fishing effort, and β is the catchability coefficient.

Given environmental stochasticity and measurement uncertainty, a stochastic modeling framework is essential. Notable studies, including [4, 5], employ SDEs to account for such complexities. Incorporating environmental noise, the fish abundance model is reformulated as:

$$dX_t = \left[rX_t\left(1 - \frac{X_t}{k}\right) - \beta X_t Y_t\right]dt + \sigma_1 dT_t, \tag{2.5}$$

where dT_t is defined in Eq (2.2), and σ_1 is a volatility parameter that captures the influence of SST variability on population dynamics.

Fishing effort is also subject to economic forces, including expected profit, operational costs (η), and a mean reversion component governed by the rate κ. Following [23], the dynamics of the fishing effort is described by:

$$dY_t = \kappa\left(\beta X_t Y_t - \eta Y_t\right)dt + \sigma_2 dW_t, \tag{2.6}$$

where σ_2 denotes the volatility of fishing effort, and $\{W_t\}_{t\geq 0}$ is an independent standard Brownian motion.

The complete system of SDEs representing the joint dynamics of fish stock, fishing effort, and SST is given by:

$$\begin{cases} dX_t = \left[rX_t\left(1 - \frac{X_t}{k}\right) - \beta Y_t X_t\right]dt + \sigma_1 dT_t, \\ dY_t = \kappa\left(\beta Y_t X_t - \eta Y_t\right)dt + \sigma_2 dW_t, \\ dT_t = \left[a\left(\theta_t - T_t\right) + \frac{d\theta_t}{dt}\right]dt + \sigma_t dB_t. \end{cases} \tag{2.7}$$

Initial conditions are specified as X_0 (initial population), Y_0 (initial fishing effort), and T_0 (initial SST). Parameter definitions are summarized in Table 1. While catch per unit effort and SST can be directly observed at specific time points, the model accounts for their underlying stochastic behavior. This system provides a rigorous framework for analyzing the influence of temperature uncertainty on fisheries dynamics. By integrating environmental and economic drivers, the model enables a more comprehensive understanding of the interactions among oceanographic conditions, fish stocks, and catch per unit effort, which are components in achieving sustainable fisheries management.

Table 1. Definition of parameters in the model.

Parameter	Definition
k	Maximum population capacity.
r	Intrinsic population growth rate.
σ_1	Volatility in stock dynamics due to temperature variability.
σ_2	Volatility in fishing effort due to economic factors.
β	Catchability coefficient.
η	Cost per unit of fishing effort.
a	Mean reversion parameter of temperature.
κ	Mean reversion parameter for catch per unit effort.

3. Estimations and predictions of the proposed model

In this section, we present the estimation of the parameters that govern the stochastic system described in Eq (2.7), together with an evaluation of the predictive accuracy of the model using empirical data from the Colombian Pacific region Figure 1. We begin by outlining the methodology used for parameter estimation, followed by the presentation of the estimated values. The predictive accuracy of the model is evaluated using the root mean square error (RMSE), which measures the average deviation between the observed values y_i and the predictions of the model $\hat{y}_i$:

$$\text{RMSE} = \sqrt{\frac{1}{n}\sum_{i=1}^{n}(\hat{y}_i - y_i)^2}, \tag{3.1}$$

where n denotes the total number of observations. Lower RMSE values indicate closer agreement between the model and the observed data. Since SDEs typically do not admit closed-form solutions, numerical methods are required to simulate their trajectories. Among these, the Euler-Maruyama method is particularly suitable due to its conceptual similarity to the classical Euler method for ordinary differential equations and its computational simplicity. This technique approximates deterministic and stochastic integrals over discrete time intervals $[t_i, t_{i+1}]$ within the domain $[0, T]$.

3.1. Temperature model estimation

To model the sea surface temperature (SST) in the study area (Figure 1), we first calculate the monthly maximum, minimum, and average SST values. The average SST is defined as follows: let $T_{\max}$ and $T_{\min}$ denote the monthly maximum and minimum SST, respectively. The average monthly SST, T, is then given by:

$$T = \frac{T_{\max} + T_{\min}}{2}. \tag{3.2}$$

Preliminary statistical analysis indicates that the average SST is normally distributed. Based on this observation, we model SST as a stochastic process using the Ornstein-Uhlenbeck framework, which incorporates mean reversion toward a time-dependent seasonal trend, as described in Eq (2.2).

3.1.1. Estimation of the mean reversion function θ_t

We begin by estimating θ_t, the deterministic mean reversion component of the Ornstein-Uhlenbeck process. This function captures the seasonal fluctuations evident in the SST time series. As shown in Figure 2, the temperature data exhibit pronounced periodic behavior. Following the methodology of [11], we model θ_t as a sinusoidal function:

$$\theta_t = A + Bt + C\sin(\omega t + \phi), \quad \text{with} \quad \omega = \frac{\pi}{6}, \tag{3.3}$$

where:

- A and B represent the intercept and linear trend, respectively;
- C is the amplitude of the seasonal cycle;
- ω is the angular frequency, calibrated to reflect annual seasonality at monthly resolution;
- ϕ is the phase shift, which aligns the function with the timing of observed seasonal peaks and troughs.

Using trigonometric identities, the model is expressed equivalently as:

$$\theta_t = A + Bt + C\left[\sin(\omega t)\cos(\phi) + \cos(\omega t)\sin(\phi)\right] \tag{3.4}$$

$$= A + Bt + D\sin(\omega t) + E\cos(\omega t), \tag{3.5}$$

where $D = C\cos(\phi)$ and $E = C\sin(\phi)$. This transformation allows the model to be estimated using linear regression with predictors $t_1 = t$, $t_2 = \sin(\omega t)$, and $t_3 = \cos(\omega t)$:

$$\theta_{t_i} = \beta_0 + \beta_1 t_1 + \beta_2 t_2 + \beta_3 t_3. \tag{3.6}$$

The parameters β_i are estimated via ordinary least squares (OLS). The original parameters of the sinusoidal function are then recovered as:

$$\begin{cases} A = \beta_0, \\ B = \beta_1, \\ \phi = \tan^{-1}\left(\frac{\beta_3}{\beta_2}\right), \\ C = \frac{\beta_2}{\cos(\phi)}. \end{cases} \tag{3.7}$$

The results of the regression analysis are presented in Table 2.

Table 2. Estimated regression parameters for the seasonal temperature model.

Coefficient	Estimate	Std. Error	t-value	p-value
β_0	27.385347	0.062234	440.036	$< 2 \times 10^{-16}$
β_1	0.000808	0.000221	3.645	0.000301
β_2	–0.615167	0.014297	–43.028	$< 2 \times 10^{-16}$
β_3	–1.889437	0.006658	–283.774	$< 2 \times 10^{-16}$

The regression yields a residual standard error of 0.0173 on 416 degrees of freedom. The coefficient of determination R^2 is 0.9988, indicating an excellent fit to the data. The adjusted R^2 remains at 0.9988,

and the model's overall significance is supported by an F-statistic of 1.201×10^5 with a corresponding p-value less than 2.2×10^{-16}.

Using the estimated regression coefficients, we recover the parameters of the seasonal function as follows:

$$\begin{cases} A = 27.385347, \\ B = 0.000808, \\ \phi = 1.256038, \\ C = -1.98706. \end{cases} \tag{3.8}$$

Thus, the final expression for the deterministic component of the SST model is:

$$\theta_t = 27.385347 + 0.000808t - 1.98706 \cdot \sin\left(\frac{\pi}{6}t + 1.256038\right).$$

This function effectively captures the observed seasonality and the long-term trend in SST. While the deterministic model describes the expected evolution of temperature over time, stochastic fluctuations are introduced through the diffusion term in Eq (2.7).

3.1.2. Estimation of the mean reversion parameter a

This subsection addresses the estimation of the mean reversion parameter a in the temperature model introduced in Eq (2.2). We now briefly review the methodology proposed by [24]. Consider a general stochastic differential equation (SDE) of the form:

$$dX_t = b(X_t, \theta)\, dt + \sigma(X_t, \theta)\, dB_t, \quad X_0 = x_0, \tag{3.9}$$

where $\theta \in \Theta \subset \mathbb{R}$ denotes the parameter vector to be estimated. It is assumed that Eq (3.9) admits a unique strong solution for all $\theta \in \Theta$, and that the diffusion coefficient $\sigma(\cdot)$ is strictly positive. Moreover, the drift and diffusion functions b and σ are assumed to be twice continuously differentiable with respect to all arguments, i.e., $b, \sigma \in C^2$.

Parameter estimation is carried out within the framework of maximum likelihood estimation (MLE), as described in [25]. Suppose that the process $\{X_t\}$ is observed at discrete time points $\{t_i\}_{i=0}^n$, with $t_0 = 0$. The likelihood function, conditional on the initial observation X_0, is given by:

$$L_n(\theta) = \prod_{i=1}^{n} f_\theta\left(t_i - t_{i-1}, X_{t_{i-1}}, X_{t_i}\right), \tag{3.10}$$

where $f_\theta(s, x, y)$ denotes the transition density of the process under parameter θ. Under standard regularity conditions, the MLE is consistent, asymptotically normal, and efficient [24].

In most practical settings, observations are collected at regular time intervals: $X_\Delta, X_{2\Delta}, \ldots, X_{n\Delta}$. If the diffusion coefficient σ is independent of θ, then the probability measures induced by the process are equivalent across values of θ. Under this assumption, the continuous-time log-likelihood function is given by [26]:

$$\hat{\ell}_t(\theta) = \int_0^t \frac{b(X_s, \theta)}{\sigma^2(X_s)}\, dX_s - \frac{1}{2}\int_0^t \frac{b^2(X_s, \theta)}{\sigma^2(X_s)}\, ds. \tag{3.11}$$

Approximating the integrals in Eq (3.11) via Itô and Riemann sums, and differentiating with respect to θ, yields the approximate score function:

$$\begin{aligned}\tilde{\ell}_n(\theta) &= \sum_{i=1}^{n} \frac{\dot{b}(X_{(i-1)\Delta}, \theta)}{\sigma^2(X_{(i-1)\Delta})} \left(X_{i\Delta} - X_{(i-1)\Delta}\right) \\ &\quad -\Delta \sum_{i=1}^{n} \frac{b(X_{(i-1)\Delta}, \theta)\, \dot{b}(X_{(i-1)\Delta}, \theta)}{\sigma^2(X_{(i-1)\Delta})},\end{aligned}$$

where $\dot{b} = \partial b/\partial\theta$.

As noted by [21], the score function $\tilde{\ell}_n(\theta)$ is biased. To address this, we consider the conditional expectation with respect to the filtration $\mathcal{F}_i = \sigma(X_\Delta, \ldots, X_{i\Delta})$. Define:

$$F_\theta(x) = \mathbb{E}[X_\Delta \mid X_0 = x], \tag{3.12}$$

which enables us to characterize the expected bias of the score function:

$$\begin{aligned}\sum_{i=1}^{n} \mathbb{E}_\theta\left[\dot{\tilde{\ell}}_i(\theta) - \dot{\tilde{\ell}}_{i-1}(\theta) \mid \mathcal{F}_{i-1}\right] &= \sum_{i=1}^{n} \frac{\dot{b}(X_{(i-1)\Delta}, \theta)}{\sigma^2(X_{(i-1)\Delta})} \left(F(X_{(i-1)\Delta}, \theta) - X_{(i-1)\Delta}\right) \\ &\quad -\Delta \sum_{i=1}^{n} \frac{b(X_{(i-1)\Delta}, \theta)\, \dot{b}(X_{(i-1)\Delta}, \theta)}{\sigma^2(X_{(i-1)\Delta})}.\end{aligned}$$

Subtracting this bias term yields the unbiased estimating function $\tilde{G}_n(\theta)$ [26]:

$$\tilde{G}_n(\theta) = \sum_{i=1}^{n} \frac{\dot{b}(X_{(i-1)\Delta}, \theta)}{\sigma^2(X_{(i-1)\Delta})} \left(X_{i\Delta} - F(X_{(i-1)\Delta}, \theta)\right). \tag{3.13}$$

Applying this estimation procedure to the temperature model (2.2), and noting that it follows an Ornstein-Uhlenbeck process, the conditional expectation is given by:

$$\mathbb{E}[T_i \mid T_{i-1}] = \theta_i + e^{-a}\left(T_{i-1} - \theta_{i-1}\right), \tag{3.14}$$

which yields the following unbiased estimating function:

$$\tilde{G}_n(a) = \sum_{i=1}^{n} \frac{\theta_{i-1} - T_{i-1}}{\sigma_{i-1}^2} \left[(T_i - \theta_i) - e^{-a}(T_{i-1} - \theta_{i-1})\right]. \tag{3.15}$$

Solving the equation $\tilde{G}_n(a) = 0$ yields the estimator $\hat{a}$ for the mean reversion parameter. Letting

$$Y_{i-1} = \frac{\theta_{i-1} - T_{i-1}}{\sigma_{i-1}^2},$$

the estimator simplifies to:

$$\hat{a} = -\log\left(\frac{\sum_{i=1}^{n} Y_{i-1}(T_i - \theta_i)}{\sum_{i=1}^{n} Y_{i-1}(T_{i-1} - \theta_{i-1})}\right). \tag{3.16}$$

Here, σ_i^2 represents the monthly variance of sea surface temperature for month i, covering the period from January 1979 to December 2012. The dataset thus comprises 420 monthly variance values. Applying the estimation method to this dataset yields the following result:

$$\hat{a} = 0.161490, \quad \text{with a standard error of } 0.00412.$$

3.1.3. Estimation of Volatility σ_t

The temperature dataset includes monthly standard deviations corresponding to the maximum, minimum, and mean sea surface temperatures (SSTs) over the study period. Additionally, for each monthly image, the standard deviation (STD) is calculated to quantify SST spatial variability across all image pixels. For example, in January 1979, the mean SST was 26.40 °C, with a corresponding STD of 0.0998 °C. The standard deviation is computed using the conventional formula:

$$\text{STD} = \sqrt{\frac{1}{n}\sum_{i=1}^{n}(T_i - \bar{T})^2},$$

where T_i denotes the SST at pixel i, and $\bar{T}$ is the mean SST across all n pixels.

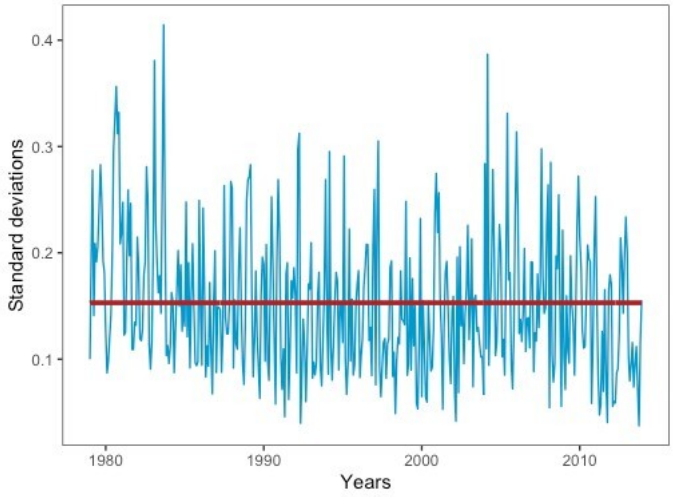

Figure 3. Monthly standard deviations of sea surface temperature, with the fitted trend line shown in red.

In Figure 3, the reported monthly standard deviations are interannual; that is, for each calendar month (e.g., January), the standard deviation of the monthly mean SST values is computed from 1979 to 2012. The observed variability in these standard deviations motivates the modeling of SST volatility as a dynamic, time-dependent process. To capture this behavior, we adopt a stochastic volatility framework based on a mean-reverting Ornstein-Uhlenbeck process.

In this framework, volatility σ_t is treated as a stochastic process exhibiting random monthly fluctuations. Consistent with the structure of Eq (2.2), its evolution is governed by the following SDE:

$$d\sigma_t = a_\sigma\,(\sigma_{\text{trend}} - \sigma_t)\;dt + \gamma_\sigma\,dB_t, \tag{3.17}$$

where σ_{trend} denotes the deterministic long-term trend of the observed volatility series. Based on the empirical data, this trend is estimated as:

$$\sigma_{\text{trend}} = 0.152565, \quad \text{with a standard error of } 0.000192.$$

Figure 3 illustrates the monthly SST standard deviations alongside the fitted trend line.

3.1.4. Estimation of the diffusion coefficient γ_σ

Following the approaches outlined in [21, 27], the diffusion coefficient γ_σ, which quantifies the magnitude of stochastic fluctuations in volatility, is estimated using the empirical quadratic variation:

$$\gamma_\sigma^2 = \frac{1}{n}\sum_{j=0}^{n-1}\left(\sigma_{j+1} - \sigma_j\right)^2, \tag{3.18}$$

where $n = 420$ is the number of monthly observations. Substituting the empirical values yields

$$\gamma_\sigma^2 = 0.006358, \quad \text{with a standard error of } 0.000312.$$

3.1.5. Estimation of the mean reversion rate a_σ

The mean reversion parameter a_σ governs the rate at which volatility returns to its long-term average σ_{trend}. As described in [21], we estimate a_σ using the following expression:

$$\hat{a}_\sigma = -\log\left(\frac{\sum_{i=1}^{n}\left(\frac{\sigma_{\text{trend}}-\sigma_{i-1}}{\gamma_\sigma^2}\right)(\sigma_i - \sigma_{\text{trend}})}{\sum_{i=1}^{n}\left(\frac{\sigma_{\text{trend}}-\sigma_{i-1}}{\gamma_\sigma^2}\right)(\sigma_{i-1} - \sigma_{\text{trend}})}\right). \tag{3.19}$$

Applying this estimator to the dataset yields:

$$\hat{a}_\sigma = 0.515815.$$

With these estimates, the volatility-related parameters of the temperature model are fully specified. In the following section, we focus on estimating the remaining model parameters, which are essential for capturing interactions among variables and for simulating the full system of SDEs (see details in [28]).

3.2. Discretized equations via the Euler–Maruyama method

In this section, we present the discretization of the continuous-time model (2.7) using the Euler–Maruyama method, with a particular focus on estimating the parameters governing species stock and catch per unit effort. The resulting discretized system is given by:

$$\begin{cases} X_{t_{j+1}} = X_{t_j} + \left[rX_{t_j} - \dfrac{rX_{t_j}^2}{k} - \beta Y_{t_j} X_{t_j}\right]\Delta t_j + \sigma_1 \Delta T_j, \\ Y_{t_{j+1}} = Y_{t_j} + \kappa\left[\beta Y_{t_j} X_{t_j} - \eta Y_{t_j}\right]\Delta t_j + \sigma_2 \Delta W_j, \\ T_{t_{j+1}} = T_{t_j} + a\left[\theta_{t_j} - T_{t_j}\right]\Delta t_j + \theta'_{t_j} + \sigma_n \Delta B_j. \end{cases} \tag{3.20}$$

Here, ΔT_j, ΔW_j, and ΔB_j denote independent standard Brownian increments. The term σ_n represents a time-varying volatility component, modeled as a discrete-time Ornstein-Uhlenbeck process:

$$\sigma_n = \sigma_{n-1} + a_\sigma(\sigma_{\text{trend}} - \sigma_{n-1}) + \delta_\sigma Z_1, \tag{3.21}$$

where $Z_1 \sim \mathcal{N}(0,1)$. The unknown parameter vector is defined as $\theta = \left(r, k, \beta, \eta, \kappa, \sigma_1^2, \sigma_2^2\right)$, and its maximum likelihood estimator is denoted by $\hat{\theta} = \left(\hat{r}, \hat{k}, \hat{\beta}, \hat{\eta}, \hat{\kappa}, \hat{\sigma}_1, \hat{\sigma}_2\right)$. Parameter estimation is conducted by applying the maximum likelihood estimation (MLE) technique to the discretized system (3.20), following the methodologies outlined in [29, 30]. Let (x_j, y_j), for $j = 1, \ldots, n$, denote the observed values of the state variables (X_j, Y_j). Assuming the process is first-order Markovian, the likelihood function takes the form:

$$L(\theta) = \prod_{j=1}^{n} f(x_j, y_j \mid x_{j-1}, y_{j-1}), \tag{3.22}$$

where $f(x_j, y_j \mid x_{j-1}, y_{j-1})$ denotes the conditional joint density of (X_j, Y_j) given (X_{j-1}, Y_{j-1}). To derive this density, consider the temperature dynamics from Eq (3.20):

$$T_{t_{j+1}} - T_{t_j} = a\left[\theta_{t_j} - T_{t_j}\right]\Delta t_j + \theta'_{t_j} + \sigma_n(B_{t_{j+1}} - B_{t_j}).$$

Assuming daily time steps (i.e., $\Delta t_j = 1$) and recognizing that B_t and W_t are independent Brownian motions with stationary increments, we obtain:

$$(B_{t_{j+1}} - B_{t_j}) \sim \mathcal{N}(0,1), \quad (W_{t_{j+1}} - W_{t_j}) \sim \mathcal{N}(0,1).$$

It follows that:

$$T_{t_{j+1}} - T_{t_j} \sim \mathcal{N}(\mu_t, \sigma_n^2),$$

and the joint process $Z_j = (X_j, Y_j)$ follows a conditional bivariate normal distribution $\mathcal{N}(\mu_j, \Sigma_j)$, depending only on the previous state $Z_{j-1} = (X_{j-1}, Y_{j-1})$, which is consistent with the Markov property.

The conditional means are:

$$\mu_{x_j} = x_j + \left[rx_j - \frac{rx_j^2}{k} - \beta y_j x_j\right], \tag{3.23}$$

$$\mu_{y_j} = y_j + \kappa\left[\beta x_j y_j - \eta y_j\right]. \tag{3.24}$$

Thus, the conditional joint density is given by:

$$f(x_j, y_j \mid x_{j-1}, y_{j-1}) = \frac{1}{\sqrt{2\pi\sigma_1\sigma_2 x_j^2 y_j^2}} \exp\left\{-\frac{1}{2}\left[\frac{(x_j - \mu_{x_j})^2}{\sigma_1^2 x_j^2} + \frac{(y_j - \mu_{y_j})^2}{\sigma_2^2 y_j^2}\right]\right\}.$$

Substituting this into the likelihood function (3.22) yields:

$$L(\theta; x_j, y_j) = \prod_{j=1}^{n} \frac{1}{\sqrt{2\pi\sigma_1\sigma_2 x_j^2 y_j^2}} \exp\left\{-\frac{1}{2}\left[\frac{(x_j-\mu_{x_j})^2}{\sigma_1^2 x_j^2} + \frac{(y_j-\mu_{y_j})^2}{\sigma_2^2 y_j^2}\right]\right\}.$$

This can be simplified to the following compact form:

$$L(\theta; x_j, y_j) = \frac{1}{(2\pi\sigma_1\sigma_2)^{n/2}\prod_{j=1}^{n} x_j y_j} \exp\left\{-\frac{1}{2}\sum_{j=1}^{n}\left[\frac{(x_j-\mu_{x_j})^2}{\sigma_1^2 x_j^2} + \frac{(y_j-\mu_{y_j})^2}{\sigma_2^2 y_j^2}\right]\right\}.$$

The corresponding log-likelihood function is:

$$\begin{aligned}\ell(\theta) = &-\frac{n}{2}\ln(2\pi) - \frac{n}{2}\ln(\sigma_1\sigma_2) - \sum_{j=1}^{n}\ln(x_j y_j)\\ &-\frac{1}{2}\sum_{j=1}^{n}\left[\frac{(x_j-\mu_{x_j})^2}{\sigma_1^2 x_j^2} + \frac{(y_j-\mu_{y_j})^2}{\sigma_2^2 y_j^2}\right].\end{aligned} \tag{3.25}$$

Parameter estimation proceeds by maximizing the log-likelihood function (3.25). This typically involves numerical optimization techniques, either gradient-based or derivative-free, over the parameter space.

Explicit parameter solutions of the model

The system of nonlinear equations, derived from the discretized model, is numerically solved to obtain estimates of the parameter vector $\hat{\theta}$. The number of observations, n, is predefined by the program. The parameter estimates are computed using the following analytical expressions:

$$\hat{r} = \frac{n\left(\alpha\zeta(\kappa - 6\nu\varrho) + \varrho(3\nu\varrho - \kappa) - \alpha^2(\zeta^2 - 4\nu\lambda)\right)}{\varphi}, \tag{3.26}$$

$$\hat{\eta} = -\frac{\alpha r n\left(\alpha^2\kappa - \alpha^2\nu\varrho + \alpha^3\zeta + 2\alpha\nu\zeta n - 2\nu^2 n\varrho\right)}{n\varphi}, \tag{3.27}$$

$$\hat{\beta} = \frac{rn\left(\alpha^2\left(\kappa + \nu\varrho - \alpha^3\zeta - 2\alpha\nu\zeta n + 2\nu^2 n\varrho\right)\right)}{\varphi}, \tag{3.28}$$

$$\hat{k} = \frac{\zeta\kappa + 4\alpha\nu\lambda - \alpha\zeta^2 - 3\nu\zeta\varrho}{4\alpha^2\lambda - 6\alpha\zeta\varrho + 2\zeta^2 n}. \tag{3.29}$$

The symbols used in these expressions are defined as follows:

$$\alpha = \sum_{i=1}^{n} x_i, \quad \nu = \sum_{i=1}^{n} x_i^2, \quad \zeta = \sum_{i=1}^{n} x_i y_i, \quad \varrho = \sum_{i=1}^{n} y_i, \quad \lambda = \sum_{i=1}^{n} y_i^2.$$

The intermediate quantities κ and φ are given by:

$$\kappa = \sqrt{\alpha^2(8\nu\lambda + \zeta^2) - 18\alpha\nu\zeta\varrho + \nu\left(-8\nu\lambda n + 9\nu\varrho^2 + 8\zeta^2 n\right)},$$

$$\varphi = 2\left(\alpha^2(2\nu\varrho^2 + \zeta^2 n) - 4\alpha^3\zeta\varrho + 2\alpha^4\lambda - 2\alpha\nu\zeta n\varrho + \nu^2 n\varrho^2\right).$$

Using these formulas, the estimated parameter values for the model (2.7) are summarized in Table 3.

Table 3. Estimated parameters of the model (2.7).

Parameter	Definition	Estimated Value
k	Maximum population capacity.	64000.861
r	Intrinsic population growth rate.	0.089176
σ_1^2	Volatility parameter for population dynamics, capturing variability due to temperature and effort interactions.	0.158927
σ_2^2	Volatility parameter reflecting variability in price associated with fishing effort.	0.000196
β	Catchability coefficient.	0.002023
η	Cost per unit of fishing effort.	3564.19
a	Mean reversion parameter for temperature.	0.161490
γ_σ^2	Diffusion parameter associated with sea surface temperature volatility.	0.006358
σ_{trend}	Long-term trend of volatility.	0.152565
a_σ	Mean reversion parameter for volatility.	0.515815
κ	Mean reversion parameter for catch per unit effort.	0.000038

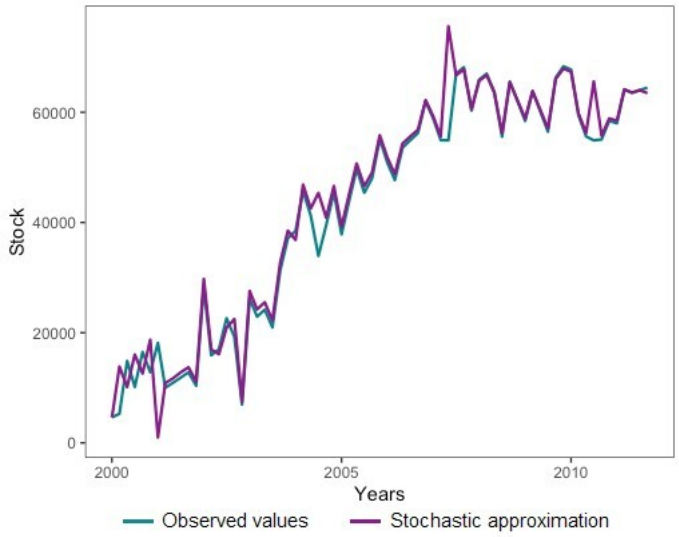

Figure 4. Comparison of observed and simulated stock values using the Euler-Maruyama method.

To evaluate model performance, subsequent analyses compare model predictions with observed data. Figure 4 depicts a comparison between observed stock values and those predicted by the stochastic model. Predictions were generated via maximum likelihood estimation using the Euler-Maruyama discretization detailed in Section 3.2. The figure demonstrates strong agreement between observed and simulated stock values, indicating that the model effectively captures

underlying population dynamics. The RMSE was computed as $RMSE = 0.029657$, reflecting a high level of concordance between the model and empirical observations.

Figure 5 compares observed catch per unit effort with simulated values obtained from the estimated model parameters, using the Euler-Maruyama discretization of system (3.20). The RMSE for catch per unit effort was 0.066680, indicating a satisfactory model fit and supporting its validity in reproducing observed patterns.

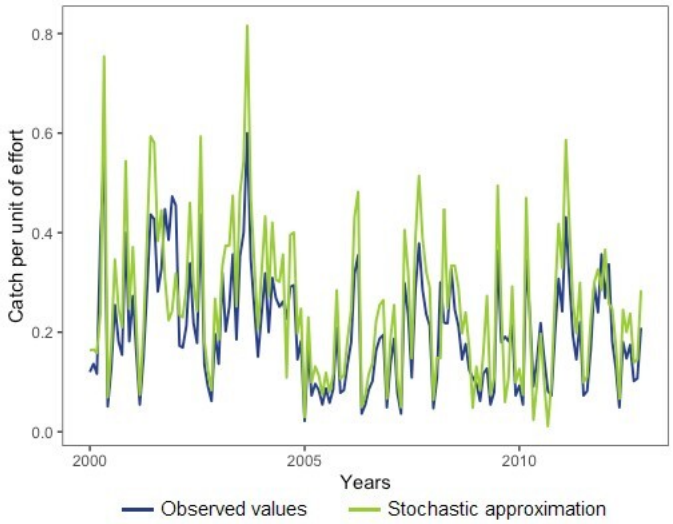

Figure 5. Comparison of observed and simulated catch per unit effort.

Parameters related to sea surface temperature were estimated assuming an Ornstein-Uhlenbeck process, discretized via Euler-Maruyama as described in Eqs (3.20) and (3.21). Simulations follow the methodology adapted from the open-source implementation by [21]. Figure 6 shows the resulting temperature trajectory. The RMSE for this model is 0.232686, indicating that the mean-reverting stochastic process provides a suitable representation of sea surface temperature dynamics.

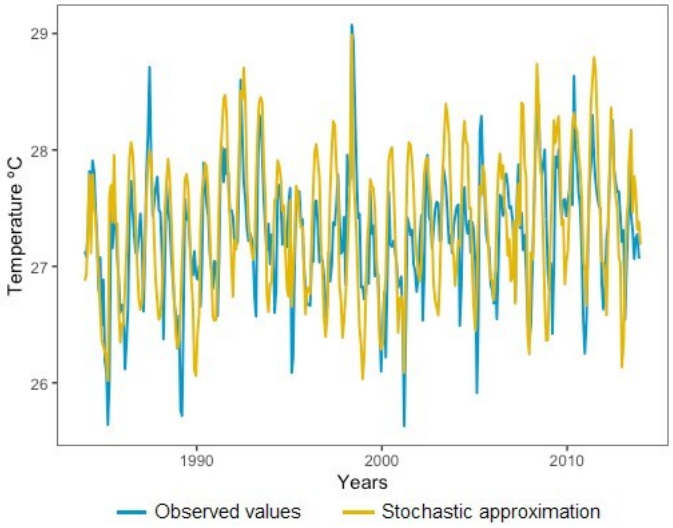

Figure 6. Comparison of observed and simulated sea surface temperatures using the Euler-Maruyama method.

To evaluate forecasting performance, the dataset is partitioned into training (70%, 2000–2008) and testing (30%, 2009–2012) subsets. Forecasts are then extended through 2015. As illustrated in Figure 7, predicted trajectories for stock (X_t), catch per unit effort (Y_t), and temperature (T_t) exhibit coherent and realistic trends. Summary statistics over the forecast period are: stock = 55,441.20 (SD = 0.359), catch per unit effort = 0.2709 (SD = 0.1645), and temperature = 28.0139°C (SD = 0.6655).

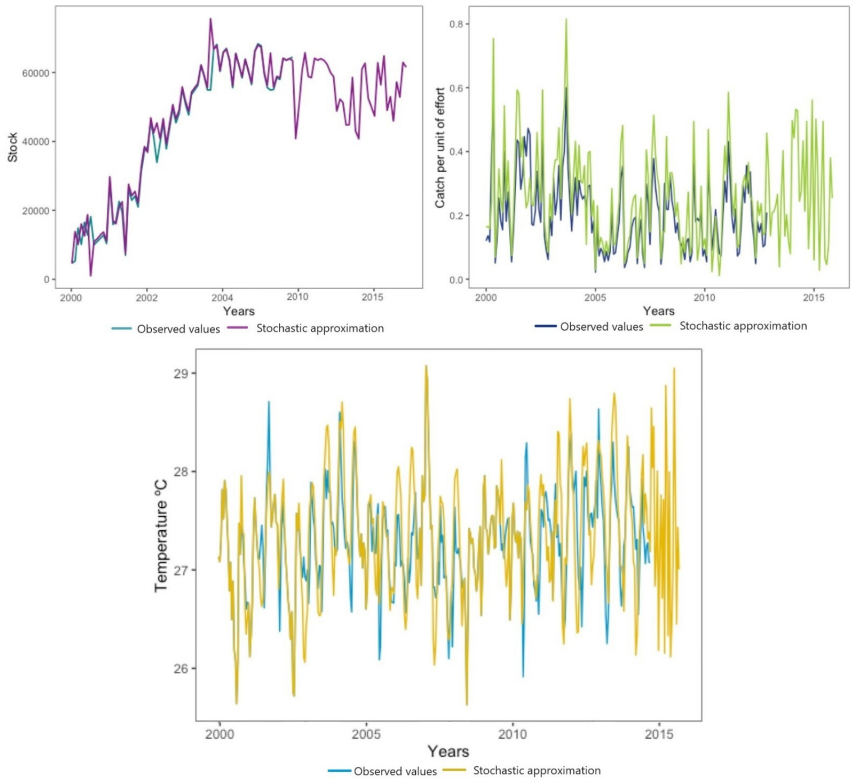

Figure 7. Forecast trajectories up to 2015 for stock, catch per unit effort, and sea surface temperature.

3.3. Confidence intervals and forecast uncertainty

To quantify the uncertainty associated with the model's forecasts, we construct confidence intervals for sea surface temperature, stock, and catch per unit effort. For the temperature process, modeled by the Ornstein-Uhlenbeck equation, a $(1-\alpha)\times 100\%$ confidence interval at time s is defined as:

$$\left(Q_{\alpha/2}(T_s), Q_{1-\alpha/2}(T_s)\right), \tag{3.30}$$

where $Q_{\alpha/2}(T_s)$ and $Q_{1-\alpha/2}(T_s)$ represent the empirical quantiles obtained from a large ensemble of simulated trajectories, each initialized at the last observed temperature value. The ensemble mean, denoted $\bar{T}_s$, is the point forecast. Figure 8 displays the 95% confidence interval for sea surface temperature over a 50-month forecast horizon. The prediction suggests that, 50 months after the last observed data point, the temperature will lie within the interval [26.5761, 27.6763].

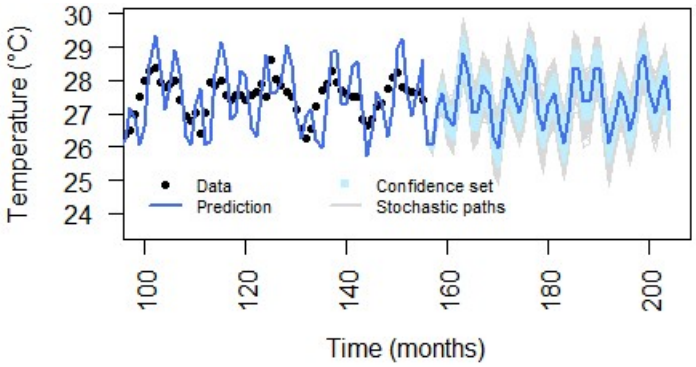

Figure 8. Forecasted sea surface temperature with 95% confidence interval, 50 months beyond the last observation.

Confidence intervals for stock and catch per unit effort are constructed using a similar approach. For the stock at time t, the 95% confidence interval is:

$$(Q_{\alpha/2}(X_t), Q_{1-\alpha/2}(X_t)),$$

where the quantiles are based on 10,000 simulated paths of the system described in Eq (3.20). The corresponding results are illustrated in Figure 9, which shows the forecasted stock dynamics over a 15-month period.

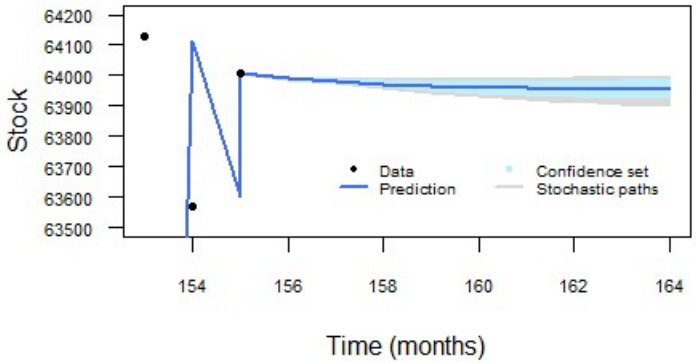

Figure 9. Forecasted stock with 95% confidence interval, 15 months beyond the last observation.

Similarly, the 95% confidence interval for catch per unit effort is given by:

$$(Q_{\alpha/2}(Y_t), Q_{1-\alpha/2}(Y_t)),$$

based on 10,000 simulations of Y_{t_j}. The forecasted interval over a 30-month horizon is shown in Figure 10. Since lower bounds of the simulated intervals may occasionally fall below zero, the interval is adjusted to ensure non-negativity, consistent with the theoretical domain of the variable. The modified interval is thus expressed as:

$$(\max\{0, Q_{\alpha/2}(Y_t)\}, Q_{1-\alpha/2}(Y_t)). \tag{3.31}$$

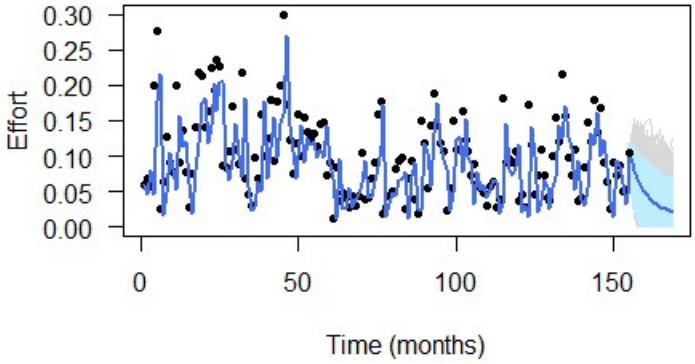

Figure 10. Forecasted catch per unit effort with 95% confidence interval, 30 months beyond the last observation.

The analysis indicates that, 15 months after the final observation, the stock is expected to lie within the interval [63,921.37, 63,999.13]. For catch per unit effort, the raw forecasted interval is $[-0.0412,\ 0.0686]$. However, given that catch per unit effort must lie in the range $[0,\ 1]$, the effective interval is adjusted to $(0,\ 0.0686)$.

3.4. Cross-validation

In this section, we assess the model's generalizability through a cross-validation procedure. A K-fold cross-validation strategy is employed, in which the dataset $\mathcal{X}$ is partitioned into $K = 10$ mutually exclusive subsets, resulting in training–validation pairs $\{\mathcal{T}_i, \mathcal{V}_i\}_{i=1}^{K}$. As discussed in [31], this approach strikes a balance between maximizing data utilization and minimizing redundancy across folds. Model hyperparameters are tuned by minimizing the RMSE, and overall model performance is evaluated using three standard metrics: RMSE, the coefficient of determination (R^2), and mean absolute error (MAE). The results of the 10-fold cross-validation are summarized in Table 4.

Table 4. Results of the cross-validation analysis.

	RMSE	**R-Squared**	**MAE**
X_t	0.6018	0.5793	0.4113
Y_t	0.0464	0.7386	0.03391
T_t	0.3327	0.6080	0.2491

RMSE quantifies the average magnitude of the prediction errors, with lower values indicating higher predictive accuracy. The R^2 values represent the proportion of variance in the observed data that is explained by the model: 57.93% for stock (X_t), 73.86% for effort (Y_t), and 60.80% for temperature (T_t). MAE offers a complementary measure by capturing the average absolute deviation between predicted and actual values. The cross-validation results suggest that the model demonstrates satisfactory predictive performance across all response variables, with particularly strong accuracy in forecasting catch per unit effort.

3.5. Sensitivity analysis

A sensitivity analysis is conducted to evaluate the impact of the estimated model parameters on the output variables. Specifically, we compute partial derivatives of the form $\partial u/\partial p$, where u denotes the model output and p represents a given parameter [32]. When u is a function of p, the derivative is given by:

$$\frac{\partial u}{\partial p} = \frac{\partial u(p)}{\partial p}.$$

The sensitivity of the model output with respect to each parameter is summarized using the normalized sensitivity index (SI), defined as:

$$SI_{u(p)} = \frac{\partial u/\partial p}{\|u/p\|} = \frac{\|p\|}{\|u\|} \cdot \frac{\partial u}{\partial p}. \tag{3.32}$$

To identify potential inflection points in the model response, the second-order derivative is also computed:

$$\frac{\partial^2 u}{\partial p^2} = \frac{\partial^2 u(p)}{\partial p^2}.$$

In addition, to explore regions indicating structural changes in model behavior, the function $u(p)$ is plotted against the estimated parameter $\hat{p}$. Figure 11 presents the results of the sensitivity analysis for four key parameters: β (catchability coefficient), r (intrinsic growth rate), k (carrying capacity), and κ (mean reversion parameter for effort).

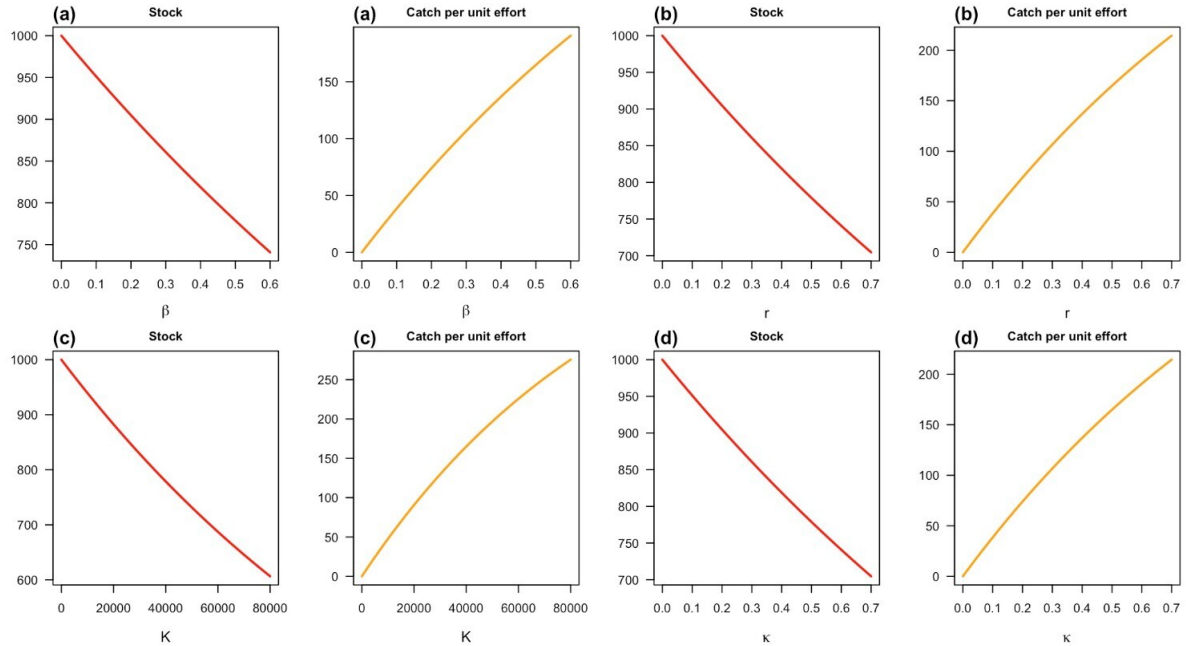

Figure 11. Sensitivity analysis of model parameters. (a) Top-left: β (catchability coefficient); (b) Top-right: r (intrinsic growth rate); (c) Bottom-left: k (carrying capacity); and (d) Bottom-right: κ (mean reversion parameter for effort).

Catchability coefficient (β): With an estimated value of $\beta \approx 0.002023$, the analysis indicates an inverse relationship between β and both stock biomass and catch per unit effort. For the range $0 \leq \beta \leq 0.6$, model outputs remain stable. However, for $\beta > 0.65$, the estimated effort becomes negative, which is biologically implausible. Therefore, the plausible range for β is $0 \leq \beta \leq 0.6$.

Intrinsic growth rate (r): Estimated at $r \approx 0.089176$, the model remains stable for $0 \leq r \leq 0.7$. Beyond this threshold, stock and effort estimates decline sharply, indicating model instability. Thus, to preserve consistency, r should be constrained within this interval.

Carrying capacity (k): With an estimated value of $k \approx 64{,}000.861$, this parameter represents the ecosystem's maximum sustainable stock. For values of $k > 80{,}000$, both stock and effort estimates deteriorate rapidly and may become negative. To ensure model stability, k should lie within the interval $0 \leq k \leq 80{,}000$.

Mean reversion parameter for effort (κ): Estimated at $\kappa \approx 0.000038$, this parameter improves the fit of the effort sub-model. The sensitivity plot shows that for $\kappa > 0.8$, stock biomass increases sharply while effort declines significantly. To avoid unrealistic projections, κ should be limited to the range $0 \leq \kappa \leq 0.7$.

4. Conclusions

We developed a stochastic modeling framework to analyze fishery resources along the Colombian Pacific Coast. By integrating SDEs with empirical ecological and environmental data, the model captures the complex interactions between biological processes (e.g., species stock dynamics) and environmental factors (e.g., sea surface temperature and catch per unit effort). The stochastic formulation incorporates inherent variability, enabling a more realistic representation of ecological dynamics over time. Model performance was evaluated using the RMSE and stochastic simulation trajectories, demonstrating strong agreement between observed and predicted values. A key contribution of this work is the introduction of a time-varying formulation for catch per unit effort, in contrast to traditional constant-effort models. Parameter estimation was conducted using the maximum likelihood method, with model discretization implemented via the Euler-Maruyama scheme to ensure both computational efficiency and numerical stability.

The model's forecasting capabilities were assessed using k-fold cross-validation, providing reliable estimates of predictive accuracy and generalizability. Confidence intervals were constructed from simulated trajectories, offering insight into forecast uncertainty. Additionally, a sensitivity analysis was performed to examine the model's responsiveness to parameter variations, an essential step for identifying influential parameters, and has practical applications in fields such as finance, ecology, and resource management. These results support model calibration and inform evidence-based policy decisions. The findings contribute to the development of data-driven strategies for fisheries management. The proposed methodology offers a practical tool for regulatory decision-making, including the formulation of sustainable fishing quotas by governmental agencies. Future work will entail incorporating additional environmental covariates, such as chlorophyll concentration, sea salinity, and surface ocean biomass by extending the model to account for spatio-temporal dynamics, thereby enhancing ecological realism and policy relevance.

Availability of data and material

The necessary code and data for achieving these results are available online at the following link https://github.com/Erika316/Stochastic_Modeling

Use of AI tools declaration

The authors declare they have not used Artificial Intelligence (AI) tools in the creation of this article.

Acknowledgments

We gratefully acknowledge the insightful comments of the anonymous reviewers, which have significantly improved the quality of the manuscript.

Conflict of interest

The authors declare there is no conflict of interest.

References

1. V. Puentes, F. Escobar, C. Polo, J. Alonso, *Estado de los Principales Recursos Pesqueros de Colombia–2014*, Autoridad Nacional de Acuicultura y Pesca–AUNAP, 2014.
2. K. Cochrane, C. De Young, D. Soto, T. Bahri, *Consecuencias del Cambio Climático Para la Pesca y la Acuicultura. Visión de Conjunto del Estado Actual de Los Conocimientos Científicos*, FAO, 2012. Available from: https://adaptecca.es/recursos/buscador/consecuencias-del-cambio-climatico-para-la-pesca-y-la-acuicultura-vision-de.
3. V. Kothandaraman, Air-water temperature relationship in Illinois river, *J. Am. Water Resour. Assoc.*, **8** (1972), 38–45. https://doi.org/10.1111/j.1752-1688.1972.tb05091.x
4. R. C. Merton, Optimum consumption and portfolio rules in a continuous-time model, *Stochastic Optim. Models Finance*, (1975), 621–661. https://doi.org/10.1016/B978-0-12-780850-5.50052-6
5. R. S. Pindyck, Uncertain outcomes and climate change policy, *J. Environ. Econ. Manage.*, **63** (2012), 289–303. https://doi.org/10.1016/j.jeem.2011.12.001
6. J. Torralba, M. Besada, A stochastic model for the Ibero-Atlantic sardine fishery. Global warming and economic effects, *Ocean Coastal Manage.*, **114** (2015), 175–184. https://doi.org/10.1016/j.ocecoaman.2015.06.023
7. T. M. Canales, M. Lima, R. Wiff, J. E. Contreras-Reyes, U. Cifuentes, J. Montero, Endogenous, climate, and fishing influences on the population dynamics of small pelagic fish in the southern Humboldt current ecosystem, *Front. Mar. Sci.*, **7** (2020), 82 https://doi.org/10.3389/fmars.2020.00082
8. L. Barboza, B. Li, M. P. Tingley, F. G. Viens, Reconstructing past temperatures from natural proxies and estimated climate forcings using short-and long-memory models, *Ann. Appl. Stat.*, **8** (2014), 1966–2001. https://doi.org/10.1214/14-AOAS785

9. F. Dornier, M. Queruel, Caution to the wind, *Energy Power Risk Manage.*, **13** (2000), 30–32.
10. D. C. Brody, J. Syroka, M. Zervos, et al., Dynamical pricing of weather derivatives, *Quantit. Finance*, **2** (2002), 189–198. https://doi.org/10.1088/1469-7688/2/3/302
11. N. C. Dzupire, P. Ngare, L. Odongo, Lévy process based Ornstein-Uhlenbeck temperature model with time varying speed of mean reversion, *Adv. Appl. Stat.*, **53** (2018), 199–224. https://doi.org/10.17654/as053030199
12. W. Swartz, R. Sumaila, R. Watson, Global ex-vessel fish price database revisited: A new approach for estimating missing prices, *Environ. Resource Econ.*, **56** (2013), 467–480. https://doi.org/10.1007/s10640-012-9611-1
13. L. M. Saavedra-Díaz, R. Pomeroy, A. A. Rosenberg, Managing small-scale fisheries in Colombia, *Marit. Stud.*, **15** (2016), 6. https://doi.org/10.1186/s40152-016-0047-z
14. A. Lindop, T. Chen, K. Zylich, D. Zeller, *A Reconstruction of Colombia's Marine Fisheries Catches*, Fisheries Centre, The University of British Columbia, 2015.
15. D. Zeller, D. Pauly, *Reconstruction of Marine Fisheries Catches for Fey Countries and Regions (1950–2005)*, Fisheries Centre, University of British Columbia, 2007.
16. P. J. Rojas-Higuera, J. D. Pabón-Caicedo, Sobre el calentamiento y la acidificación del océano mundial y su posible expresión en el medio marino costero colombiano, *Revista Acad. Colomb. Cienc. Ex. Fis. Nat.*, **39** (2015), 201–217. https://doi.org/10.18257/raccefyn.135
17. Food and Agriculture Organization, *Consecuencias del Cambio Climático Para la Pesca y la Acuicultura*, 2012.
18. E. H. Allison, A. L. Perry, M. C. Badjeck, W. Neil Adger, K. Brown, D. Conway, et al., Vulnerability of national economies to the impacts of climate change on fisheries, *Fish Fish.*, **10** (2009), 173–196. https://doi.org/10.1111/j.1467-2979.2008.00310.x
19. J. J. Selvaraj, V. Arunachalam, K. V. Coronado-Franco, L. V. Romero-Orjuela, Y. N. Ramírez-Yara, Time-series modeling of fishery landings in the Colombian Pacific Ocean using an ARIMA model, *Reg. Stud. Mar. Sci.*, **39** (2020), 101477. https://doi.org/10.1016/j.rsma.2020.101477
20. N. M. Razali, Y. B. Wah, Power comparisons of Shapiro–Wilk, Kolmogorov-Smirnov, Lilliefors and Anderson-Darling tests, *J. Stat. Model. Anal.*, **2** (2011), 21–33.
21. P. Alaton, B. Djehiche, D. Stillberger, On modelling and pricing weather derivatives, *Appl. Math. Finance*, **9** (2002), 1–20. https://doi.org/10.1080/13504860210132897
22. A. Aguilar, Z. Malpica, B. Urbina, *Dinamica de Poblaciones de Peces*, primera edición, Libertad, 1995.
23. N. H. Shah, B. M. Yeolekar, Optimal fish harvesting with deterioration, effort and price-sensitive demand, *Adv. Appl. Math.*, **1** (2016), 124–131. https://doi.org/10.22606/jaam.2016.12005
24. M. Kessler, A. Lindner, M. Sørensen, *Statistical Methods for Stochastic Differential Equations*, 1st Edition, Chapman and Hall/CRC, New York, 2012.
25. P. J. Bickel, K. A. Doksum, *Mathematical Statistics: Basic Ideas and Selected Topics*, 1st Edition, Chapman and Hall/CRC, New York, 2015.

26. B. M. Bibby, M. Sørensen, Martingale estimation functions for discretely observed diffusion processes, *Bernoulli*, (1995), 17–39. https://doi.org/10.2307/3318679

27. I. Basawa, B. Prakasa Rao, *Statistical Inference for Stochastic Processes*, Academic Press, (1980).

28. E. Martínez-Salinas, Un Modelo Estocástico Para Analizar Los Efectos de la Variación de la Temperatura Sobre la Captura Pesquera a lo Largo de la Costa del Pacífico Colombiano, Master's thesis, Universidad Nacional de Colombia, 2020).

29. P. Aguirre, E. González-Olivares, S. Torres, Stochastic predator-prey model with allee effect on prey, *Nonlinear Anal. Real World Appl.*, **14** (2013), 768–779. https://doi.org/10.1016/j.nonrwa.2012.07.032

30. A. Ríos-Gutiérrez, S. Torres, V. Arunachalam, Studies on the basic reproduction number in stochastic epidemic models with random perturbations, *Adv. Differ. Equations*, **288** (2021), 1–24. https://doi.org/10.1186/s13662-021-03445-2

31. E. Alpaydin, *Introduction to Machine Learning*, MIT Press, 2020,

32. L. Arriola, J. M. Hyman, Sensitivity analysis for uncertainty quantification in mathematical models, in *Mathematical and Statistical Estimation Approaches in Epidemiology*, Springer, (2009), 195–247.